ISSN 1063-7826, Semiconductors, 2015, Vol. 49, No. 7, pp. 953–958. © Pleiades Publishing, Ltd., 2015.
Original Russian Text © N.S. Kurochkin, A.A. Vashchenko, A.G. Vitukhnovsky, P.N. Tananaev, 2015, published in Fizika i Tekhnika Poluprovodnikov, 2015, Vol. 49, No. 7, pp. 975–980.

AMORPHOUS, VITREOUS, AND ORGANIC SEMICONDUCTORS

Effect of the Length of Ligands Passivating Quantum Dots on the Electrooptical Characteristics of Organic Light-Emitting Diodes

N. S. Kurochkin[a, b], A. A. Vashchenko[a, b]*, A. G. Vitukhnovsky[a, b, c], and P. N. Tananaev[d]

[a] *Lebedev Physical Institute, Russian Academy of Sciences, Moscow, 119991 Russia*
[b] *Moscow Institute of Physics and Technology, Dolgoprudny, 141700 Russia*
[c] *National Research Nuclear University "MEPhI", Moscow, 115409 Russia*
[d] *Dukhov Research Institute of Automation, Moscow, 101000 Russia*
**e-mail: andrewx@mail.ru*

Submitted December 9, 2014; accepted for publication December 15, 2014

Abstract—The electrooptical characteristics of organic light-emitting diodes with quantum dots passivated with organic ligands of different lengths as emitting centers are investigated. It is established that the thickness of the ligand coating covering the quantum dots has little effect on the Förster energy transfer in the diodes, but significantly affects the direct injection of charge carriers into the quantum-dot layer. It is shown that the thickness of the passivation coating covering the quantum dots in a close-packed nanoparticle layer is determined both by the length of passivating ligands and the degree of quantum-dot coverage with ligands.

DOI: 10.1134/S1063782615070155

1. INTRODUCTION

The electroluminescence of organic compounds was observed for the first time in 1953 by A. Bernanose and his colleagues, who observed the emission of light upon the application of a high ac (alternating current) voltage to thin films of acriquine and acridine orange. However, the era of organic light-emitting diodes (OLEDs) began in earnest in 1987, when C. Tang of Eastman Kodak Company discovered the bright electroluminescence of tris(8-hydroxyquinoline) aluminum (Alq_3) in a double-layer structure containing, apart from the Al complex, a triaryldiamine hole-transport layer [1].

The search for new materials led to the creation of OLEDs based on semiconductor nanocrystals, or quantum dots (QDs), for the first time synthesized by colloidal-chemistry methods in 1993 [2]. This QD-OLED technology has been actively developed over the past two decades. The benefits of using QDs for OLED fabrication are related to their narrow-band luminescence, photophysical stability, and the convenience of varying the emission wavelength by varying the QD size [3, 4]. Colloidal QDs which are presently most commonly used in OLEDs consist of a core and one or more shells of different semiconductors. These QDs feature a higher fluorescence quantum yield and are less susceptible to adverse external factors. Furthermore, the QDs are coated with organic ligands in the process of their synthesis to make possible their dispersion in a solvent.

It was shown in several recent publications that the chemical nature and the length of passivating ligands have a considerable impact on the characteristics of QDs [5, 6], and this, in turn, affects the properties of OLEDs fabricated on their basis. In particular, it was demonstrated in [5] that, by changing the length of the ligands, one can control the exciton diffusion length in the QD layer, while changing the chemical nature of ligands may result in considerable variations in the conduction- and valence-band energies in QDs [6]. At the same time, little work has been carried out on the influence of the length of passivating ligands of the same chemical nature on the characteristics of devices based on highly luminescent QDs (see, e.g., [7]).

Here, we investigate CdSe/CdS/ZnS QDs stabilized by ligands of different lengths and study the effect of the thickness of the ligand layer coating the QDs on the characteristics of OLEDs fabricated on their basis.

2. EXPERIMENTAL

The QD-OLEDs under study were fabricated from well-known organic compounds *N*,*N*'-diphenyl-*N*,*N*'-bis(3-methylphenyl)-[1,1'-diphenyl]-4,4'-diamine (TPD), poly(3,4-ethylenedioxythiophene) polystyrene sulfonate (PEDOT:PSS), and aluminum 8-hydroxyquinolinate (Alq_3). They served as the hole-transport layer (TPD), hole-injection layer (PEDOT:PSS), and electron-transport layer (Alq_3).

Three-layer CdSe/CdS/ZnS colloidal QDs (core/shell/shell structure) were synthesized by Nanotech–Dubna Ltd. using methods similar to those described in [8, 9]. In such QDs (see Fig. 1), the top of the valence band of the core lies above the valence bands of the shells, and the bottom of the conduction

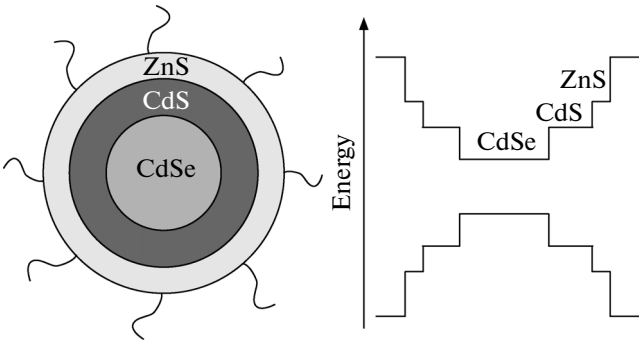

Fig. 1. Schematic layout of a CdSe/CdS/ZnS (core/shell/shell structure) quantum dot stabilized with organic ligands and the qualitative outline of its energy-band diagram.

band of the core lies below the conduction bands of the shells. This gives a number of advantages in comparison to QDs without semiconductor shells. First, the electron and hole wavefunctions are localized in the core, which increases the probability of their recombination within the core, while the probability of nonradiative decay of surface states is reduced. Thus, the quantum yield of the QD photoluminescence increases [3]. Second, the shells protect the active core of the nanoparticle from adverse external factors, such as, molecules of water and oxygen, which cause degradation of the semiconductor material [10]. The ligand molecules coating the QD also increase its photostability. The band gap of this coating organic material is much wider than the band gap of the QD core and shells, which is important for QD-OLED operation. Ligands with both folded and linear structure were used for QD stabilization. They included oleylamine ($C_{18}H_{35}NH_2$), whose molecule is folded due to the presence of a double bond; octylthiol ($C_8H_{17}SH$); and dodecanethiol ($C_{12}H_{23}SH$). The coating of QDs with octylthiol and dodecanethiol was carried out by replacing the original oleylamine ligand upon prolonged stirring of the dispersion of initial QDs in a surplus of the corresponding alkylthiol and subsequent repeated purification of the QDs by reprecipitation with alcohols.

The nanoparticles were studied using absorption and fluorescence spectrometry, transmission electron microscopy (TEM), and scanning electron microscopy (SEM). The QD photoluminescence quantum yield was determined with respect to Rhodamine 6G solution in ethanol (η = 95%) using the method described in [11]. According to these measurements, the quantum yield is the same for all three types of QDs (the difference is smaller than 5%) independent of the type of passivating ligand and is ~60%. Solutions with the same QD concentrations were prepared by monitoring their absorption spectra and taking into account the fact that, according to the Bouguer–Lambert–Beer law, the absorption is proportional to the concentration. The photoluminescence and absorption spectra of the solutions and films were measured using a Perkin Elmer LS45 spectrofluorometer and Perkin Elmer Lambda 45 spectrophotometer, respectively.

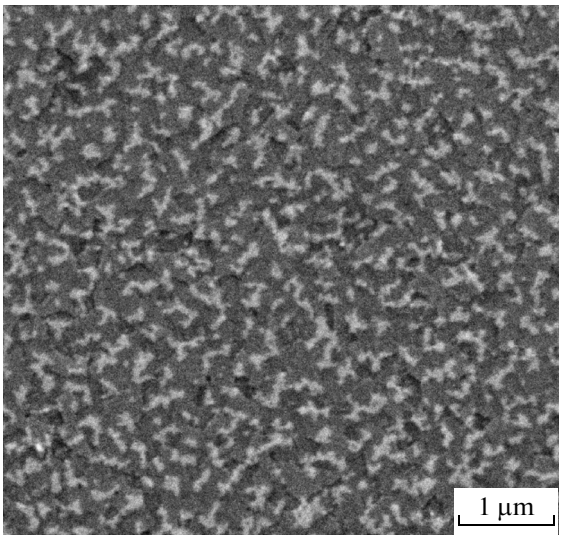

Fig. 2. SEM image of QDs on the surface of TPD. QDs with octylthiol ligands are shown as an example. Brighter regions correspond to nanoparticles aggregated into a so-called island structure. The surface coverage with QDs is 20–25%.

The OLED samples were fabricated using centrifugation and thermal evaporation and consisted of the following layers: substrate/ITO/PEDOT:PSS/TPD/QD layer (partial surface coverage)/Alq_3(30 nm)/Al(100 nm). The PEDOT:PSS layer was deposited by centrifugation from an aqueous solution using an MTI TC 100 spin coater rotating at 2000 rpm. The QDs and TPD were deposited simultaneously from a toluene solution (50 μL) at the same rotation speed. The SEM data (Fig. 2) confirm that phase segregation of the QDs under study and TPD takes place; this behavior was observed back in 2002 for double-layer QDs with other stabilizer ligands [12]. the remaining layers, i.e., the Alq_3 and aluminum layers, were deposited using a Leybold–Heraeus Univex 300 system at a pressure below 2×10^{-5} Torr.

The OLED spectra were measured using an ASEQ Instruments LR1 spectrometer. The OLED current–voltage characteristics were recorded in a few seconds in an automatic mode under computer control.

3. EXPERIMENTAL RESULTS

TEM images of QDs stabilized by different ligands are shown in Fig. 3. One can see that, similarly to their behavior on the surface of TPD, the nanoparticles aggregate into island structures on the surface of the grid for TEM measurements.

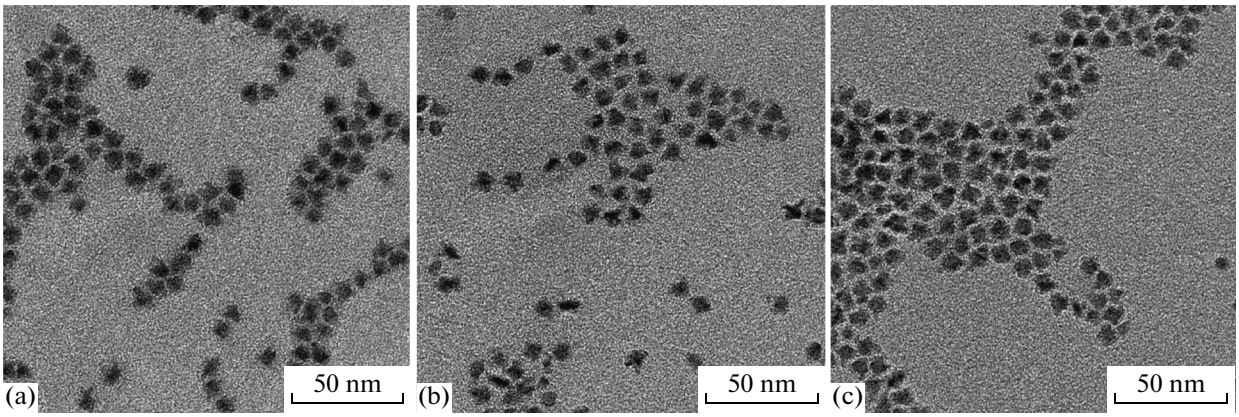

Fig. 3. TEM images of QDs with (a) octylthiol, (b) oleylamine, and (c) dodecanethiol ligands.

The spacings between adjacent QDs within an island occur because of the presence of passivating ligands, which have a looser structure than the QDs. This spacing, which we relate to the effective thickness of the ligand shell (assumed in the following to be half the spacing between the QDs), is determined both by the ligand length and by factors depending on the nanoparticle-synthesis conditions. Estimates of the QD spacings for each case are listed in the table. One can see that, for QDs coated with oleylamine, the ligand layer is thicker than for QDs coated with octylthiol and dodecanethiol. Looking now at the chemical formulas of the ligands, one can see that, for the QDs under study, the thickness of the ligand layer very tentatively correlates with the ligand length determined by the number of carbon atoms in the chain. Thus, in the samples with octylthiol and dodecanethiol ligands, the average spacing between the QDs is almost the same in spite of the fact that these molecules have different lengths. It is possible that this is the result of a difference in the degree of QD coverage with ligands. Since it seems impossible to directly measure the latter quantity, which, furthermore, may vary uncontrollably during nanoparticle synthesis, the only appropriate method for estimating the QD concentration in a closely-packed layer is to use direct measurement by electron-microscopy techniques.

Another characteristic determined from the TEM images is the QD distribution with respect to the diameters of their inorganic body (i.e., disregarding the ligand length). As one would expect, this distribution is the same, within error limits, for QDs with different types of ligand and is represented by a Gaussian peak with an average diameter of ~7.5 nm and 10% dispersion.

It is known that there are two main mechanisms of exciton formation in QDs incorporated into QD-OLEDs [13]: the direct injection of charge carriers into the QDs and Förster energy transfer from the transport layers, whose molecules play the role of exciton donors. According to [13], excitons mostly form in the Alq_3 electron-transport layer in the vicinity of the Alq_3/QD interface. It was found previously for single-layer QDs that the contribution of the direct-injection mechanism to luminescence depends considerably on the effective thickness of the ligand coating covering the QDs and falls exponentially as this thickness increases [14]. In our previous work [15], it was also shown that the probability of the Förster energy transfer can be heavily dependent on the distance R between the QD layer and the exciton-donor layer. Thus, the probability of energy transfer via the Förster mechanism from a donor molecule near the interface between the Alq_3 and the QD layer to the latter is proportional to $(R_F/R)^6$; here, R_F is the Förster radius, characterizing the distance at which efficient energy transfer from an organic molecule to a QD takes place. Therefore, an increase in R by 1 nm upon the replacement of octylthiol with oleylamine (see table) can lead to a considerable reduction in the Förster energy-transfer rate.

To find out how the type of ligand affects the contribution of the Förster mechanism to luminescence in QD-OLEDs, we studied the photoluminescence spectra of isolated layers of Alq_3, QDs (Fig. 4a), and QD/Alq_3 (Fig. 4b) deposited onto glass. The structure of these layers was the same as in subsequently fabricated QD-OLEDs.

Spacing between adjacent QDs upon coating with different ligands

Ligand	Average spacing, nm	Standard deviation, nm
Oleylamine	3.6	0.5
Octylthiol	2.7	0.6
Dodecanethiol	2.8	0.5

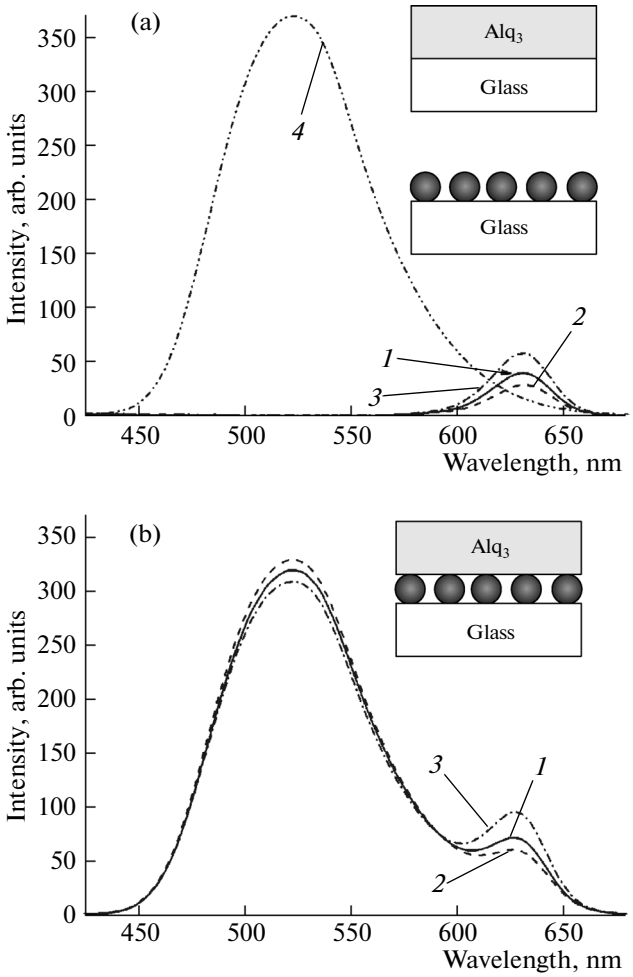

Fig. 4. Photoluminescence spectra of (a) glass/QD and (b) glass/QD/Alq_3(30nm) structures containing QDs coated with (*1*) oleylamine, (*2*) octylthiol, and (*3*) dodecanethiol ligands. Curve *4* in panel (a) shows the photoluminescence spectrum of a glass/Alq_3 sample (30 nm). The insets show the schematic layouts of the structures.

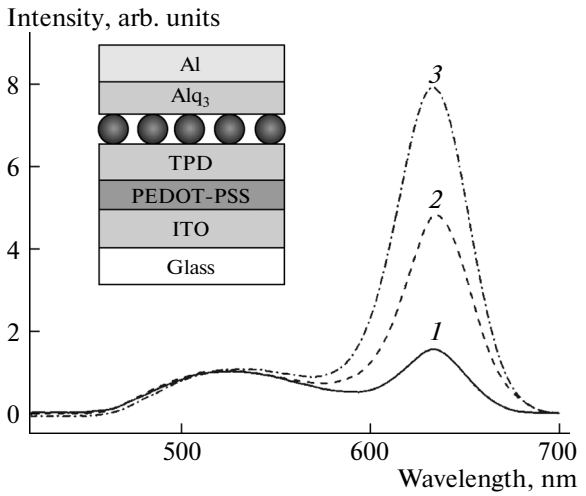

Fig. 5. Normalized electroluminescence spectra of QD-OLEDs containing QDs coated with (*1*) oleylamine, (*2*) octylthiol, and (*3*) dodecanethiol molecules; the voltage $V = 6.8$ V. The inset shows the schematic layout of the OLED.

The glass/QD structures were fabricated by centrifugation. The concentration of nanoparticles in the solutions prepared for this purpose was adjusted to be the same for each QD type. The glass/QD/Alq_3(30 nm) structures were fabricated by the sputtering of Alq_3 onto the glass/QD samples after measurements with the latter had been carried out. According to Fig. 4a, the photoluminescence spectra of layers of QDs with different ligands differ in intensity, even though they were deposited from solutions with equal nanoparticle concentrations and the photoluminescence quantum yield for different QDs is the same. We attribute this discrepancy to differences in the amount of nanocrystals on the substrate, which results from inaccuracy of the dropper upon spin-coating deposition of the QD films. Upon evaporation of the Alq_3 layer, the intensity of the QD luminescence increased by 40–55%, while the intensity of the luminescence from Alq_3 was 10–15% lower as compared to the glass/Alq_3 sample. Since the absorption in the films is small (not exceeding 5% of the incident radiation), reabsorption processes can be disregarded. Thus, changes in the luminescence intensity are explained by the Förster transfer of excitons from the 30-nm Alq_3 layer to the layer of nanocrystals. Within measurement error, these changes are independent of the length of the passivating ligands. Apparently, in the case under study, the distance R between the QD layer and the Alq_3 donor molecules is shorter than the critical length R_F, and the efficiency of the energy transfer between the donor and acceptor [16] (which characterizes the fraction of generated excitons that are transferred to the QDs) $E = 1/[1 + (R/R_F)^6]$ varies insignificantly with an increase in the ligand-coating thickness. As a result, the rate of the Förster transfer of excitons from the Alq_3 layer to the QDs does not change noticeably as well.

To compare the characteristics of QD-OLEDs based on QDs with different thicknesses of the ligand layer, we fabricated a series of three OLEDs with QDs coated with oleylamine, octylthiol, and dodecanethiol. The concentration of nanoparticles in the solutions used for OLED fabrication was the same in all three cases and coincided with that in the above-described photoluminescence experiments.

The electroluminescence spectra of the fabricated OLEDs normalized to the Alq_3-emission peak at 525 nm are shown in Fig. 5. The narrower emission peak at 635 nm corresponds to the QDs. Evidently, the relationship between the peaks of the QD and the Alq_3 emission changed in favor of QDs in comparison to

the photoluminescence spectrum. This behavior can be explained both by the contribution from additional mechanisms of QD excitation (direct charge-carrier injection and Förster energy transfer from the TPD transport layer) and by narrowing of the exciton-generation region in Alq_3 in the case of electroluminescence as compared to photoluminescence. As was said above, excitons mostly form in Alq_3 at the interface with the QD layer and, thus, it can be stated, as it was with photoluminescence, that the efficiency of the Förster energy transfer varies insignificantly upon a change in the passivating ligand length. The spectra also indicate that the relative contribution from the emission of QDs is larger for diodes based on nanoparticles with short octylthiol and dodecanethiol ligand molecules as compared to the OLED containing QDs with relatively long oleylamine molecules.

The current–voltage characteristics I–V of the OLEDs are plotted on the double-logarithmic scale in Fig. 6. They confirm the effect of passivation QD coatings on charge transport in organic structures. One can see that, for the same voltages, the QD-OLEDs with the longest oleylamine molecules have the lowest working currents, while those with the shortest octylthiol molecules have the highest. We note also that the I–V curves of all three diodes feature two distinct regions corresponding to different current-flow conditions: the ohmic mode, in which the current density j is proportional to the voltage V, and the mode of trap-limited current, in which $j \propto V^n$ ($n > 2$) [17].

We attribute the differences in the current–voltage characteristics and the spectra of the OLEDs based on QDs with octylthiol and dodecanethiol, where the thicknesses of the ligand coatings are nearly the same, to inaccuracy of the dropper upon the spin-coating deposition of the nanoparticle films leading to differences in the degree of substrate coverage with nanoparticles. The smaller working currents for OLEDs containing QDs with dodecanethiol molecules give evidence of a higher nanoparticle concentration in the layer (QDs represent a barrier for charge carriers), which is in agreement with the spectra of the diodes. Meanwhile, the current–voltage characteristics and spectra of OLEDs containing QDs with oleylamine molecules can be understood only by taking into account differences in direct injection, which is much less efficient in nanocrystals with a thick oleylamine coating.

Thus, we conclude that the thickness of the QD ligand coating has little effect on the Förster energy transfer in QD-OLEDs, but considerably affects the direct injection of electrons and holes into the QDs. To obtain OLEDs with high working currents (and, consequently, high brightness) and cleaner emission from the QDs, one should use nanoparticles coated with a thinner layer of short ligand molecules (provided that such a coating does not affect the QD characteristics, such as the photoluminescence quantum yield).

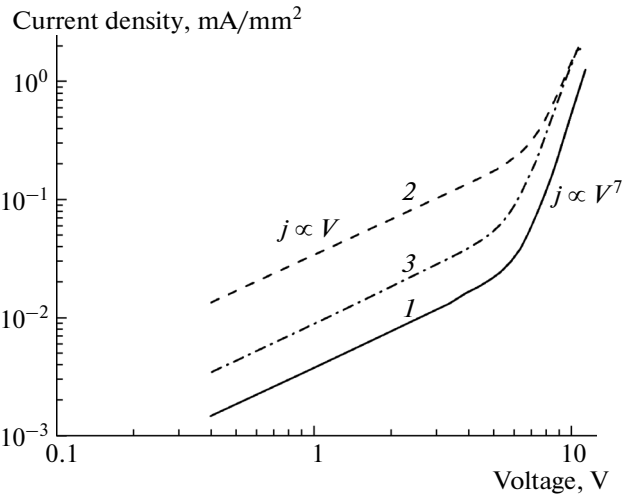

Fig. 6. Current–voltage characteristics of QD-OLEDs containing QDs coated with (*1*) oleylamine, (*2*) octylthiol, and (*3*) dodecanethiol molecules.

4. CONCLUSIONS

Thus, we have demonstrated that the thickness of the passivation coating of a QD in a close-packed QD layer is not unambiguously determined by the ligand length. The QD spacing can be considerably affected by the degree of QD coverage with ligands and, thus, direct electron-microscopy measurements are required to estimate the QD concentration in a close-packed layer. It is established that, for CdSe/CdS/ZnS QDs, the thickness of the passivation coating has a considerable effect on the electroluminescence in QD-OLEDs. To enhance electroluminescence resulting from the direct injection of charge carriers, it is necessary to choose passivators with the shortest molecules.

ACKNOWLEDGMENTS

We are grateful to S.A. Ambrozevich (LPI) for his help and consultations and A.A. Lizunova (MIPT) for her help with microscopy measurements.

REFERENCES

1. C. W. Tang and S. A. VanSlyke, Appl. Phys. Lett. **51**, 913 (1987).
2. C. B. Murray, D. J. Norris, and M. G. Bawendi, J. Am. Chem. Soc. **115**, 8706 (1993).
3. J. Lim, W. K. Bae, J. Kwak, S. Lee, C. Lee, and K. Char, Opt. Mater. Express **2**, 594 (2012).

4. R. B. Vasil'ev and D. N. Dirin, *Quantum Dots: Synthesis, Properties, Application* (FNM, Moscow, 2007) [in Russian].
5. G. M. Akselrod, F. Prins, L. V. Poulikakos, E. M. Y. Lee, M. C. Weidman, A. J. Mork, A. P. Willard, V. Bulovic, and W. A. Tisdale, Nano Lett. **14**, 3556 (2014).
6. P. R. Brown, K. Donghun, R. R. Lunt, N. Zhao, M. G. Bawendi, J. C. Grossman, and V. Bulovic, ACS Nano **8**, 5863 (2014).
7. A. M. Munro, J. A. Bardecker, M. S. Liu, Y.-J. Cheng, Y.-H. Niu, I. J.-L. Plante, A. K.-Y. Jen, and D. S. Ginger, Microchim. Acta **160**, 345 (2008).
8. J. Z. Niu, H. Shen, C. Zhou, W. Xu, X. Li, H. Wang, S. Lou, Z. Du, and L. S. Li, Dalton Trans. **39**, 3308 (2010).
9. H. Shen, H. Wang, Z. Tang, J. Z. Niu, S. Lou, Z. Du, and L. S. Li, Cryst. Eng. Commun. **11**, 1733 (2009).
10. P. Reiss, M. Protiere, and L. Li, Small **5**, 154 (2009).
11. J. N. Demasa and G. A. Crosby, Phys. Chem. **75**, 991 (1971).
12. S. Coe, W.-K. Woo, M. Bawendi, and V. Bulovic, Nature **420**, 800 (2002).
13. P. O. Anikeeva, PhD Thesis (Massachusetts, USA, MIT, 2009), p. 46.
14. Y. Liu, M. Gibbs, J. Puthussery, S. Gaik, R. Ihly, H. W. Hillhouse, and M. Law, Nano Lett. **10**, 1960 (2010).
15. A. A. Vashchenko, V. S. Lebedev, A. G. Vitukhnovskii, R. B. Vasiliev, and I. G. Samatov, JETP Lett. **96**, 113 (2012).
16. P. R. Selvin, Nature Struct. Mol. Biol. **7**, 730 (2000).
17. Z. Chen, B. Nadal, B. Mahler, H. Aubin, and B. Dubertre, Adv. Funct. Mater. **24**, 269 (2013).

Translated by M. Skorikov